

ORIGINAL ARTICLE



Adhesive bonding of secondary steel components for offshore wind turbines

Matthias Albiez¹ | Jakob Boretzki¹ | Thomas Ummenhofer¹

Correspondence

Dr.-Ing. Matthias Albiez
Karlsruhe Institute of Technology
KIT Steel and Lightweight Structures,
Research Center for Steel,
Timber and Masonry
Otto-Ammann-Platz 1
76131 Karlsruhe
Email: matthias.albiez@kit.edu

¹ KIT Steel and Lightweight Structures,
Karlsruhe, Germany

Abstract

Offshore wind turbines consist of the main components tower, nacelle and rotor blades. Additionally, numerous secondary components are connected to the primary structure. These include amongst others boat landings, platforms, cable protection tubes and corrosion protection systems. Usually, these elements are connected to the primary structure by welding or bolts. Both joining techniques reduce the fatigue performance of the primary structure by inducing geometric and/or metallurgical notches. In contrast, by fastening the secondary components by adhesive bonding, no geometric or metallurgical notches are induced in the primary structure. Furthermore, the bonding can be carried out directly on the coating. In contrast to welded or bolted joints, adhesively bonded joints require a differing geometry that allows large bonding areas. This paper highlights the results of experimental investigations regarding the load bearing behaviour of adhesively bonded secondary components under a combination of lateral load and bending varying different geometrical parameters.

Keywords

Offshore structures, hollow sections, secondary components, joining technology, adhesive bonding, adhesive, experimental testing, load bearing behavior

1 Introduction

1.1 Secondary steel in offshore wind structures

Load-bearing structures of offshore wind turbines have a large number of secondary steel components such as cable protection tubes, ladders, boat landings, service platforms or corrosion systems (see Figure 1). The secondary components are currently connected to the primary structure at the manufacturing site by welding or bolted connections. Both joining methods result in geometric and/or metallurgical notches. This leads to a required reduction in the FAT class of the primary structure during fatigue design and thus often to increased wall thicknesses. In addition, specific aspects of corrosion protection (e.g. contact corrosion) must be considered for both welded and bolted connections.

During the service life of offshore structures, in situ fastening of secondary components is frequently required. This is particularly challenging in terms of durable design and fabrication in accordance with corrosion protection requirements. In addition, subsequent welding or bolting leads to a modification of the primary structure and often necessitates a redesign of the load bearing structure taking into account the new structural boundary conditions.



Figure 1 Offshore wind energy plant with secondary steel structures. Source: Mark Leybourne, CC BY 2.0, edited [1]

Adhesive bonding offers an alternative joining technique solution without the aforementioned challenges. The temperatures reached during the adhesive bonding process do not lead to harmful heat input into the primary structure, thus avoiding metallurgical notches. In particular, the 2K epoxy coatings frequently used in the offshore industry

have a high adhesive strength on steel substrates. Therefore, it is often possible to bond directly to the coated steel surface. In this case, only the corrosion protection of the secondary component is necessary. Nevertheless, due to the strength properties of adhesives and adhesive bonds a constructive design suitable for bonding is required, resulting in circular connecting plates to allow large bonding areas (see Figures 2/3).

1.2 FOSTA project P 1393

The investigation of adhesive bonding of components under water [2-5] as well as under offshore conditions and for offshore structures [6, 7] is the subject of current research activities. In the recently completed IGF research project "Offshore bonding" of the Forschungsvereinigung Stahlanwendung e.V. (P 1393) [8], the main research focus was on bonded secondary components in different exposure zones (splash water, water change and underwater zones). Based on the application specific requirements, suitable adhesives were selected and characterized. Then, various adhesives were subsequently selected and characterized. In the next step, a manufacturing concept suitable for offshore use is developed and validated. Experimental investigations of the load-bearing and failure behavior after aging on both outdoor weathered in the North Sea and laboratory-aged specimens represent a research focus not detailed within this paper. The quasi-static testing of adhesively bonded components on a real scale is used to validate the manufacturing concept and the mechanical strength. Finally, the manufacturing concept is tested by divers under real conditions in the port of Rostock. An overview of the work carried out in the project is detailed in [9].

1.3 Scope of this paper

As part of research project P 1393 [8], detailed investigations were carried out to develop an adhesive bonding manufacturing process for secondary steel components. The tests on manufacturing and aging behavior were performed on small-scale specimens. A further focus was the development, optimisation and validation of the geometry and manufacturing process of secondary fasteners on a large scale, detailed in [10]. This paper presents an excerpt of these investigations and focuses on experimental investigations on large-scale adhesively bonded secondary steel components for three different interactions of bending moment and transversal load and two different fastener geometries.

2 Materials and test specimen

The specimens designed for the bending tests consist of two joining parts: firstly, the fastener, which consists of a hollow circular section (CHS) with a welded end plate, and secondly, a square base plate, representing the primary structure. The two components are joined by a two-dimensional adhesive bond between the end plate and the base plate (Figure 3). Two different geometries are experimentally investigated. Both the end plate diameter and the cross section of the CHS differ between these geometries. According to the geometry of the end plate, the dimensions of the base plate are also adapted. Furthermore, the length of the fastener CHS respectively the distance between the load introduction point and the adhesive bond

is varied in order to have different interactions of lateral force and bending moment loading. The dimensions of the specimens can be seen in Figure 2. The circular hollow sections are hot-finished circular hollow sections according to DIN EN 10025-1 made of S355J2. The end plates are sections of round steel according to DIN EN 10060, also made of S355J2. The sections of the base plates are made of heavy plate S355J2 according to DIN EN 10029. For the smaller geometry, the welded joint between the CHS and the end plate is made by a circumferential, combined HV/fillet weld with a dimension of 6 mm. This is necessary due to the limited space on the end plate, the high wall thickness of the CHS and the loads to be expected. The connection for the larger geometry is made by a circumferential fillet weld with a dimension of 10 mm.

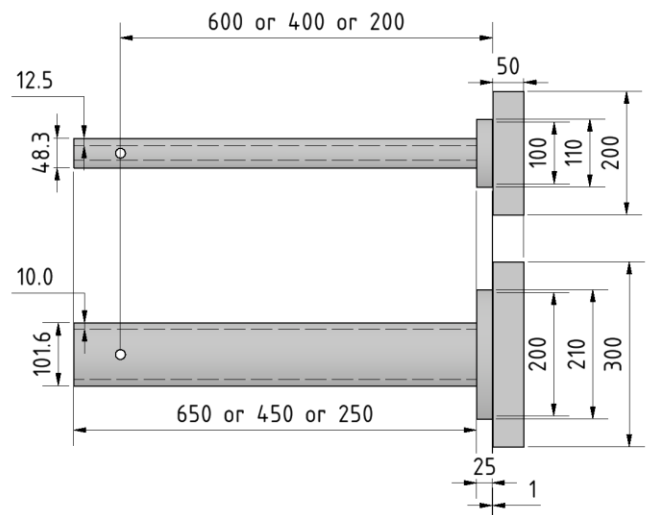


Figure 2 Test specimen for bending tests, above: small geometry, below: large geometry; all dimensions in [mm] [10]

Based on the results of the durability tests, bonding is carried out on coated surfaces. For this purpose, the surfaces of the parts to be joined are coated with the epoxy-based coating system Hempadur 35620 from Hempel. The coating is applied in three layers of 200 μm each. The specimen presented in this paper are bonded with the epoxy resin adhesive SikaPower-1200 from Sika AG.

3 Manufacturing of the adhesively bonded joint

Due to bonding on epoxy-coated substrates, surface pre-treatment is significantly simplified compared to bonding on blank steel. The surfaces of the joining parts are cleaned only with towels to remove coarse dirt. Circular sealing elements (butyl cord or VHB tape) are subsequently applied to seal the sides of the bonding area. The adhesive is applied by injection into the cavity between the end plate of the fastener and the primary structure (base plate). For this purpose, two injection holes are drilled in the end plate of the fastener, into which hose nozzles are inserted and the injection hoses are subsequently connected. The distance between the end plate and the base plate is adjusted using distance pieces. The next step is to align and assemble the joining parts. First, isopropanol is injected into the cavity to clean and degrease the joining surfaces. For the large geometry, 100 ml is injected. For the small geometry, 50 ml is injected. After injection, the isopropanol remains in the adhesive joint for 1 minute. The isopropanol is then blown out with oil-free compressed air.

The pressure is 5 bar, the blow-out time is 1 minute for the large geometry and 20 seconds for the small geometry. After completion of the cleaning process, adhesive injection can be carried out as the next manufacturing step. For both adhesives, a compressed air-driven cartridge press is used for this purpose. The pressure is set to 5 bar. Injection is carried out until the outlet hose is filled with adhesive over a few centimetres. It was found that the temperature of the adhesive and the joining parts has a considerable influence on the viscosity of the adhesive. With increasing viscosity, the injection time increases considerably. Thus, when selecting the adhesive system, the ambient and joining part temperature must be taken into account for the specific application. The specimens are then cured at room temperature until testing. The time between production and testing for all test specimens is above the recommended curing time of two days at 23° ambient temperatures.

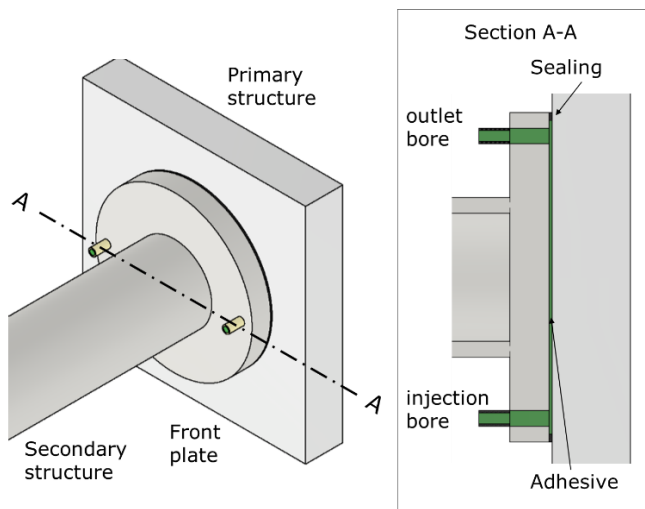


Figure 3 Construction detail and manufacturing concept of adhesively bonded secondary steel component

4 Experimental testing

The cantilever tests of the bonded specimens are carried out on a servo-hydraulic 1000 kN machine. A specific testing device is developed for the connection to the clamping field. This is shown in Figure 4. The load is applied via steel plates, which are connected to the CHS of the fastener using a load application bolt. At the top end of the steel plates there is a steel block which connects the two plates. This block is connected to the piston of the testing machine. For the smaller specimen with a smaller CHS diameter, a narrower block is used to minimize the bending stress on the load application bolt. The tests are carried out displacement controlled. The displacement speed is determined depending on the cantilever length. For the short cantilever of 0.2 m, the test speed is 1 mm/min, for the medium cantilever (0.4 m) 2 mm/min and for the long cantilever (0.6 m) 3 mm/min. The displacement is increased linearly for all specimens until the specimen fails. In addition to recording machine force and machine displacement, a local measuring of the relative displacement between the end plate of the fastener and the base plate is made in vertical and horizontal direction. These local measurements are used to determine the deformations in the bonded joint.

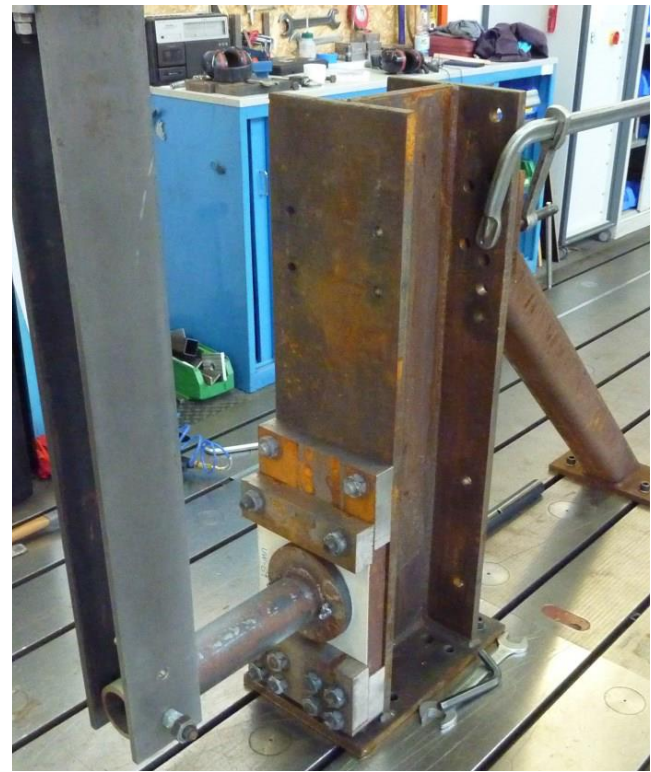


Figure 4 Test setup bending tests

5 Results and discussion

The results of the bending tests are first presented in the form of diagrams in which the recorded force is plotted over the machine displacement. A differentiation is made between large and small fastener geometries according to Figure 2. Figure 5 first shows the load-displacement curves of the fastener geometry with an end plate diameter of 200 mm. It can be seen for all tests that the force increases almost linearly until just before the maximum load is reached. The failure is announced by a slight reduction in stiffness shortly before the maximum load is reached. The failure of the adhesively bonded joint occurs abruptly for all tests. The fastener detaches completely from the base plate. The mean values of the recorded maximum loads are summarised in Table 1. In addition, it can be seen that a larger lever arm is accompanied by a decrease in the maximum load. The observed increase in machine deformation with bigger lever arm lengths can be attributed to the elastic deformation of the connecting component. The results of the inductive displacement transducers are not presented at this point. The measured values for all measuring points are less than 0.1 mm even when the maximum load is reached. Since the measuring accuracy of the selected measuring equipment is approximately in this order of magnitude, an evaluation of the values is not expedient.

An analysis of the fracture patterns of the specimen with an end plate diameter of 200 mm (see Figure 6) shows that cohesive failure of the coating occurs over a large area at the base plate and in smaller areas in the coating of the endplate of the fastener. Cohesive failure of the adhesive layer is found only in small areas at the transition between the above described large coating failure areas.

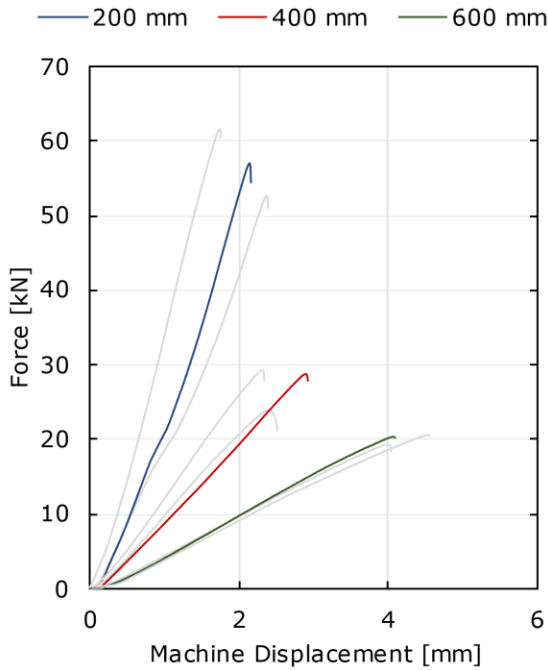


Figure 5 Load-displacement behaviour of all specimens with end plate diameter of 200 mm in bending tests, exemplary graph coloured, others grey

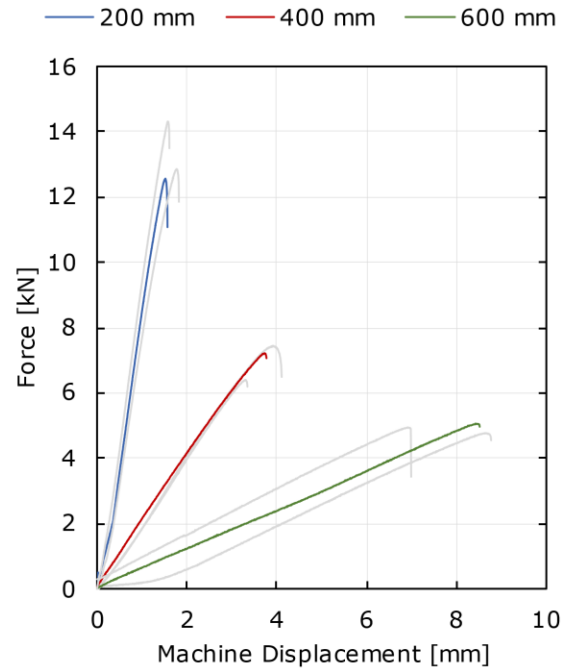


Figure 8 Load-displacement behaviour of all specimens with end plate diameter of 100 mm in bending tests, exemplary graph coloured, others grey

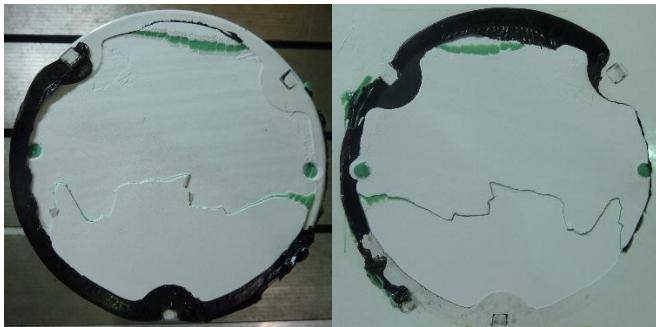


Figure 6 Exemplary fracture patterns for fasteners with end plate diameter of 200 mm

The load-deformation behaviour of the small fastener geometry with an end plate diameter of 100 mm is qualitatively comparable. For these test series, the load-deformation behaviour is also linear for all specimens (cf. Figure 9). Failure is announced by a small decrease in stiffness. Due to increasing lever arm, the maximum loads are reduced and the machine paths at maximum load are higher.



Figure 7 Exemplary fracture patterns for fasteners with end plate diameter of 100 mm

As expected, the considerably smaller bonding surface due to the smaller end plate diameter results in reduced maximum loads of the bonded joint. Figure 7 shows exemplary fracture patterns of specimens with the end plate diameter of 100 mm. Cohesive failure in the coating at the base and end plate also dominates the failure for this fastener geometry.

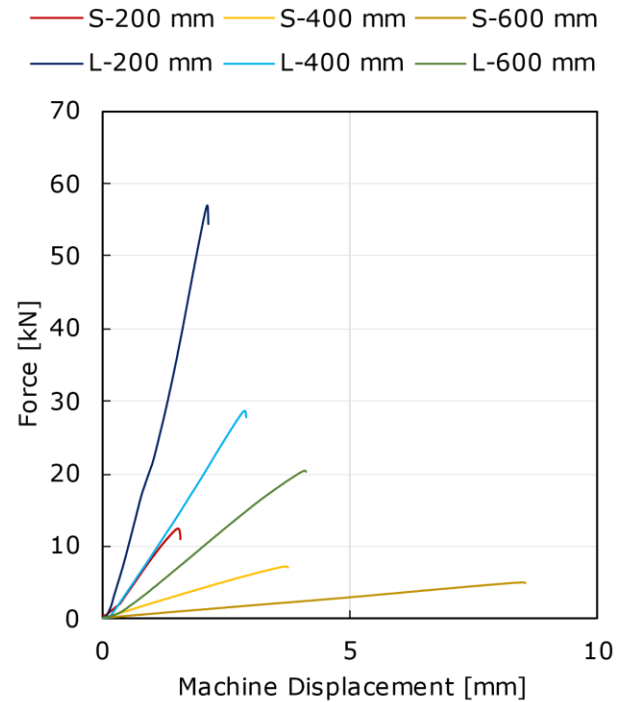


Figure 9 Summary of exemplary load-displacement curves for all test series

Figure 9 summarises the experimental results displaying one representative load-deformation curve for each test series and clarifies the described correlations between end plate diameter, lever arm length and load bearing behaviour. A summary of the mean values of all experimentally determined maximum loads for each test series presented in this study is given in Table 1. A comparison of the tests carried out shows that bonded fasteners can be manufactured reliably and exhibit reproducibly high load capacities. The coefficient of variation of the maximum load is only 7.7 % on average across all test series. A comparison of the test series with the same geometry of the bonded connection but different lever arms shows that the maximum load decreases with increasing lever arm. However, if the bending moment acting in the bonded joint is considered, a different correlation can be observed. The bending moment at maximum load is almost comparable for all three lever arms (see Table 1). For the parameter field investigated, the applied bending moment is therefore to be regarded as the reason for the failure of the adhesive joint. The influence of the additional shear force stress seems to be of secondary importance in this case.

Table 1 Mean values of maximum loads and corresponding bending moments of all test series

Test series	Lever arm length [mm]	Maximum load [kN]	Bending moment in adhesive bond [kNm]
Small geometry (D = 100 mm)	200	13.25 ± 0.95	2.65 ± 0.19
	400	7.00 ± 0.54	2.80 ± 0.22
	600	4.92 ± 0.15	2.95 ± 0.09
Large geometry (D = 200 mm)	200	57.15 ± 4.51	11.43 ± 0.90
	400	27.25 ± 2.91	10.90 ± 1.17
	600	20.05 ± 0.72	12.03 ± 0.43

A detailed and in-depth numerical analysis of the experimental tests at the stress level, fully described in [10], shows that the maximum transverse tensile stresses orthogonal to the adhesive layer are of a comparable size for all three lever arms. These show stress values just above the nominal bond strength of the coating, which was determined using an Elcometer (~ 20 MPa). A comparable relationship is observed for the small fastener geometry.

6 Conclusions

Within the context of a recently completed FOSTA research project, a methodology for the adhesive bonding of secondary steel components in offshore wind turbines was developed and systematically investigated. This paper presents results on experimental investigations on component-like secondary components. In principle, it is shown that the adhesive bond can be manufactured reliably using the developed injection method. The joining gap is completely filled for all investigated specimens. In addition, failure generally occurs in the coating and no adhesive failure of the adhesive layer occurs, which confirms the suitability of the surface pretreatment applied in the manufacturing process. The adhesively bonded connection

exhibits a high load-bearing capacity. For the large fastener geometry, bending moment capacities of more than 10 kNm are obtained. The connection exhibits high stiffness. The maximum relative displacement between the joined parts is less than 0.1 mm. In the considered range, there is no influence of the shear force on the bending moment load capacity. A subsequent numerical modelling shows that the failure of the specimen generally occurs when the transverse tensile stresses in joining layer locally exceed the value of 20 MPa. This value agrees with the nominal adhesive tensile strength of the coating used.

Funding

The project IGF 20836 BG (P 1393) of the Forschungsvereinigung Stahlanwendung e.V., Sohnstraße 65, 40237 Düsseldorf, is supported by the Federal Ministry for Economic Affairs and Climate Action through the German Federation of Industrial Research Associations as part of the program for promoting industrial cooperative research.

References

- [1] Mark Leybourne, Thanet Offshore Wind Farm, 16. Juni 2015, Lizenz: Attribution 2.0 Generic.
- [2] Blumentritt, B.; Glück, N.; Flügge, W. (2019) *Halteungen im Unterwasserbereich klebtechnisch fügen (Teil 1)*. Adhäsion Kleben & Dichten, no. 6/2019.
- [3] Blumentritt, B.; Glück, N.; Flügge, W. (2019) *Halteungen im Unterwasserbereich klebtechnisch fügen (Teil 2)*. Adhäsion Kleben & Dichten, no. 7-8/2019.
- [4] Li, S.; Ma, C.; Hou, B.; Liu, H. (2022) *Rational design of adhesives for effective underwater bonding*. Frontiers in Chemistry. Vol. 10, 1007212.
- [5] Myslicki, S.; Kordy, H.; Kaufmann, M. et al.: *Under water glued stud bonding fasteners for offshore structures*. International Journal of Adhesion and Adhesives 98 (2020), 102533.
- [6] Albiez, M. et al. (2022) *Hybrid joining of jacket structures for offshore wind turbines – Determination of requirements and adhesive characterization*. Engineering Structures 259, 114186.
- [7] Albiez, M. et al. (2022) *Hybrid joining of jacket structures for offshore wind turbines – Validation under static and dynamic loading at medium and large scale*. Engineering Structures 259, 113595.
- [8] Flügge, W. et al. (2023) *Steigerung der Festigkeit und Dauerhaftigkeit von Stahl-Klebungen im Offshorebereich*. Forschungsvereinigung Stahlanwendung e. V. (FOSTA P 1393, IGF Nr. 20836 BG), final report.
- [9] Boretzki, J. et al. (2023) *Klebtechnischer Anschluss von Sekundärbauteilen bei Offshore-Bauwerken*. Adhäsion Kleben & Dichten, no. 4/2013.
- [10] Albiez, M.; Boretzki, J. (2023) *Manufacturing process and load-bearing behaviour of adhesively bonded steel secondary components in offshore structures*, submitted to Ocean Engineering.